Drug Testing and Analysis

WILEY

RESEARCH ARTICLE

Identification of Metabolites for the Novel 5α-Reductase Inhibitor Epristeride In Vitro and Its Potential Impact on Doping Testing

Zhongquan Li[1] | Bing Liu[1] | Yirang Wang[1] | Jiahui Cheng[1] | Rodrigo Aguilera[2] | Xiaojun Deng[1] | Qing Chen[3] | Peijie Chen[1,4]

[1]Research Institute for Doping Control, Shanghai University of Sport, Shanghai, China | [2]Drug Control Centre, Department of Analytical, Environmental and Forensic Sciences, School of Cancer and Pharmaceutical Sciences, Faculty of Life Sciences and Medicine, King's College London, London, UK | [3]Department of Pharmacy, Shenyang Medical College, Shenyang, China | [4]School of Exercise and Health, Shanghai University of Sport, Shanghai, China

Correspondence: Bing Liu (liubing2019@sus.edu.cn) | Qing Chen (chenqing.0906@163.com) | Peijie Chen (chenpeijie@sus.edu.cn)

Received: 11 February 2025 | **Revised:** 20 August 2025 | **Accepted:** 18 October 2025

Funding: This work was supported by the Ministry of Science and Technology of the People's Republic of China (2020YFF0304500), the Research Project of Shanghai University of Sport (2025STD004), and the World Anti-Doping Agency (252C03BL).

Keywords: 5α-reductase inhibitor | CYP450 enzyme | epristeride | microsome | molecular docking

ABSTRACT

Epristeride, a novel noncompetitive inhibitor of Type II 5α-reductase, has emerged as a potential therapeutic alternative for benign prostatic hyperplasia (BPH). Given that other 5α-reductase inhibitors, such as finasteride and dutasteride, are already monitored for their potential impact on doping control, comprehensive metabolic studies of epristeride are crucial for antidoping. This study investigates the metabolic pathways and metabolites of epristeride using in vitro microsome models, offering preliminary insights into the pharmacokinetics of this drug. Metabolite profiling was performed using liquid chromatography–high resolution mass spectrometry (LC-HRMS), with data acquisition facilitated by Xcalibur 4.2 software and metabolite identification facilitated by Compound Discoverer 3.3. By employing network pharmacology, the potential targets of epristeride are predicted. The binding energy is calculated using AutoDock Vina software to predict its impact on steroid metabolism. The study proposed three primary metabolites of epristeride: two Phase I oxidation products (M1 and M2) and one Phase II glucuronidation product (M3). Pathway analysis revealed that among the five CYP450 isoforms examined, CYP3A4 played a dominant role. The docking results tentatively elucidated five key target proteins (ESR1, CYP19A1, STAT3, AKR1C3, and CYP17A1) with low binding energies, indicating stable interactions. Notably, Phase I metabolites (M1 and M2) showed significant binding potential with these targets, whereas the Phase II metabolite (M3) exhibited lower binding stability. These findings provide a detailed understanding of epristeride's metabolic pathways and its potential biological impacts, offering valuable insights for monitoring its presence as a confounding factor in doping control.

Zhongquan Li, Bing Liu, Yirang Wang, and Jiahui Cheng contributed equally to this work.

1 | Introduction

5α-reductase inhibitors are primarily classified into Types I and II categories and further divided into competitive and noncompetitive inhibitors based on their mechanisms of action. These drugs primarily function by inhibiting 5α-reductase activity, thereby reducing the conversion of testosterone (T) to dihydrotestosterone (DHT), which effectively lowers DHT levels. They are commonly used to treat conditions associated with elevated DHT, such as benign prostatic hyperplasia (BPH) and androgenetic alopecia (AGA) [1–3]. Finasteride and dutasteride are the two main 5α-reductase inhibitors with distinct mechanisms of inhibition. Finasteride is a selective Type II 5α-reductase inhibitor that significantly reduces DHT levels in both serum and tissues and is commonly used in the treatment of BPH and AGA [4, 5]. In contrast, dutasteride inhibits both Types I and II 5α-reductase, leading to a more comprehensive reduction in DHT levels and demonstrating particularly strong efficacy in treating BPH [6, 7]. Additionally, epristeride, a novel noncompetitive type II 5α-reductase inhibitor [8, 9], has been approved in China under the brand names "Aipuliete" and "Chuanliu" for the treatment of BPH. Epristeride is known for its high selectivity and rapid onset of action, with significant increases in peripheral blood testosterone levels observed after 6 weeks of continuous treatment [10]. Consequently, epristeride offers an effective alternative for patients who are unable to tolerate finasteride or dutasteride.

Compared with finasteride and dutasteride, the noncompetitive inhibition mechanism of epristeride suggests that its effect on 5α-reductase may not be fully predicted based on existing data from the other two drugs. Competitive inhibitors such as finasteride and dutasteride directly compete with testosterone at the enzyme's active site, whereas epristeride binds at a different site, thereby modulating enzyme activity without competing for substrate binding [5, 6]. This distinction implies that epristeride could produce different inhibitory dynamics and potentially distinct alterations in androgen metabolism. The World Anti-Doping Agency (WADA) has introduced an Athlete Biological Passport (ABP) with a steroidal module, which is intended for the monitoring of longitudinal profiles of an athlete's steroid variables in urine to identify endogenous anabolic androgenic steroids that are administered exogenously [11, 12]. In doping control, alongside monitoring the testosterone (T) to epitestosterone (E) ratio in urine ($T/E > 4$), it is also crucial to analyze endogenous steroids, including 5α-reductase metabolites such as dihydrotestosterone (DHT) and androsterone (A) [13, 14]. Administration of 5α-reductase inhibitors, such as dutasteride, leads to a decrease in the excretion of 5α-reduced steroids, whereas the excretion of 5β-reduced steroids may remain unaffected, resulting in a lowered ratio of 5α- to 5β-reduced steroids [14]. Studies have shown that dutasteride administration can suppress the urinary levels of 5α-reduced metabolites for up to 8 days, whereas the T/E ratio remains unaffected [1], adding complexity to doping control interpretations. Notably, 5α-reductase inhibitors like finasteride and dutasteride can also alter the isotopic composition of steroid metabolites, which may significantly impact gas chromatography combustion isotope ratio mass spectrometry analyses [15]. To prevent athletes from masking the use of performance-enhancing drugs, both finasteride and dutasteride are considered confounding factors of the steroid profile by WADA [16]. However, the use of epristeride has not yet been approved by the US Food and Drug Administration (FDA) or other European regulatory bodies [17], and the metabolic characteristics of the drug and its metabolites are still not fully understood. These studies are critical for the evaluation and clinical application of the drug.

Hepatic and cutaneous biotransformation play critical roles in the elimination of both endogenous and exogenous compounds, including drugs [18]. Liver microsomes are a commonly utilized enzymatic system for assessing metabolic stability, as they are rich in key drug-metabolizing enzymes (DMEs), including the cytochrome P450 (CYP) family and uridine 5′-diphospho-glucuronosyltransferase (UGT) enzymes [19–21]. CYP3A4 is a critical member of the CYP family, widely expressed in the liver and small intestine and is responsible for metabolizing approximately 50% of clinically used drugs [22–24]. Its activity is regulated by various factors, including genetic polymorphisms [25], drug induction, and inhibition [26]. CYP3A4 has an extensive substrate range, encompassing antibiotics (e.g., erythromycin), antifungal agents (e.g., fluconazole), anticancer drugs (e.g., cyclophosphamide), and analgesics (e.g., acetaminophen) [27, 28]. This broad substrate specificity highlights the critical role of CYP3A4 in drug–drug interactions. Similarly, skin microsomes serve as an important site for local drug metabolism and the detoxification of endogenous compounds. As the body's largest organ, the skin exhibits unique biotransformation capabilities due to its enzymatic diversity and barrier functions. Although CYP3A4 is present in skin microsomes, its activity is generally lower than that in hepatic microsomes. Other CYP enzymes, such as CYP1A1 and CYP2E1, are more prominent in the skin and play pivotal roles in local drug metabolism and detoxification [29]. These enzymatic activities not only influence the therapeutic effects of topically applied drugs but may also affect the systemic bioavailability of exogenous compounds absorbed through the skin.

In studies on 5α-reductase inhibitors, finasteride undergoes Phase I metabolism primarily via CYP3A4, producing ω-hydroxyfinasteride, which is subsequently converted into glucuronide conjugates by UGT enzymes. As early as 1994, researchers tentatively elucidated Phase I metabolites such as ω-hydroxyfinasteride and 6α-hydroxyfinasteride in male rat hepatic microsomes [30]. In humans, the primary urinary metabolite of finasteride is carboxy finasteride, whereas the parent drug accounts for less than 1% of urinary excretion [31, 32]. Consequently, WADA uses carboxy finasteride as a biomarker in urine to detect finasteride use with a reporting level of 5 ng/mL. Dutasteride is metabolized mainly by CYP3A4 and CYP3A5 in vivo, producing multiple active metabolites [33]. Because epristeride has structural similarities to finasteride, it is hypothesized that epristeride may exhibit comparable biotransformation pathways.

This study employed human liver *microsomes* (HLMs) and minipig skin *microsomes* (SMs) models to explore the in vitro metabolism of epristeride, providing foundational insights for further research on its in vivo metabolic pathways. Skin

microsomes were included as a complementary model, because the skin also expresses drug-metabolizing enzymes and may provide insights into potential extrahepatic metabolism. To further enhance the understanding of epristeride's pharmacological and metabolic mechanisms, a network pharmacology approach was employed by integrating bioinformatics tools and molecular docking simulations [34, 35]. This innovative methodological approach was expected to provide a comprehensive perspective on epristeride's pharmacological mechanisms and address critical considerations for its regulation in antidoping strategies.

2 | Materials and Methods

2.1 | Reagents and Solutions

Pooled human liver microsomes (pHLMs; 0.1 mol/L phosphate buffer, pH 7.4; protein concentration, 20 mg/mL), Skin S9 Fraction (Male; 150 mM KCl; 250 mM sucrose; protein concentration, 4 mg/mL), nicotinamide adenine dinucleotide phosphate (NADPH) regeneration solution A (1.3 mmol/L NADP+, 3.3 mmol/L $MgCl_2$, and 3.3 mmol/L 6-phosphoglucose), NADPH regeneration solution B (0.4 U/mL 6-phosphoglucose dehydrogenase and 0.05 mmol/L sodium citrate), UDP-glucuronosyltransferase (UGT) incubation system (5 mmol/L uridine diphosphoglucuronic acid [UDPGA], 5 mmol/L D-glucarboxylic acid-1,4-lactone, and 25 μg/mL alamethicin), and PBS buffer (0.1 mol/L, pH 7.4) were provided by IPHASE BIOSCIENCE Co. Ltd. (Suzhou, China). The standard of epristeride was provided by MedChemExpress (New Jersey, United States). Acetonitrile (HPLC grade) was purchased from Sigma-Aldrich (St. Louis, MO, United States), methanol (HPLC grade) and DMSO were purchased from Merck KGaA (Darmstadt, Germany), and formic acid (analytical grade, 98%) was purchased from Fluka (Charlotte, North Carolina, United States). Water was purified using a Milli-Q Advantage A10 ultrapure water system (Millipore, Massachusetts, United States).

Five cytochrome P450 (CYP) isoforms—CYP2D6, CYP2C9, CYP1A2, CYP2B6, and CYP3A4—were selected for metabolic pathway studies. The corresponding selective inhibitors were quinidine (10 mM), sulfaphenazole (1 mM), α-naphthoflavone (200 μM), sertraline (25 mM), and ketoconazole (1 mM), all purchased from IPHASE BIOSCIENCE Co. Ltd. (Suzhou, China).

2.2 | Preparation of HLMs

Epristeride was dissolved in DMSO to prepare a 1.0 mg/mL stock solution, and then, 1 μL of this solution was added to the newly prepared system solution to make the final volume reach 200 μL (including 162 μL buffer, 10 μL NADPH regeneration solution A, 2 μL NADPH regeneration solution B, 20 μL UDPGA solution, and 5 μL liver microsomes). The mixed system was incubated at 37°C for 1 h, and 600-μL precooled acetonitrile was added to terminate the reaction. After centrifugation at 12,000 rpm for 10 min, the supernatant was transferred to a glass liner tube and waited for analysis. At the same time, control groups were set up: blank solution, incubation reaction system solution without target drug, reaction system solution without liver microsomes, and reaction system solution without regeneration system to ensure the validity of the results.

2.3 | Preparation of Skin Microsomes

For the skin microsome experiments, 25 μL of skin microsomes was used to replace the liver microsomes, and the buffer volume was adjusted to 142 μL. All other procedures were performed consistently with those typically used in the liver microsome experiments.

2.4 | Preparation of Enzyme Inhibition

An additional system solution was prepared by combining 1 μL of epristeride stock solution and 1 μL of selective inhibitor, adjusting the final volume to 200 μL (including 181-μL buffer, 10-μL NADPH regeneration solution A, 2-μL NADPH regeneration solution B, and 5-μL liver microsomes). The mixed system was incubated at 37°C. The incubation reaction times for the CYP450 enzyme subtypes vary depending on the specific enzyme. For CYP-2D6 and CYP-3A4, the reaction time was 10 min, whereas CYP-2C9 requires 20 min. CYP-1A2 and CYP-2B6 both require longer incubation periods of 30 min, and then, 600 μL of precooled acetonitrile was added to terminate the reaction. Subsequent operations were the same as above. The control group analysis of this system comprised a blank solution, an incubation reaction system solution without selective inhibitor, and a reaction system solution without regeneration system.

2.5 | Liquid Chromatography–High Resolution Mass Spectrometry Parameters

Metabolite separation was performed using a Thermo Vanquish LC system (Thermo Fisher, Bremen, Germany) equipped with an ACE-EXCEL C18-PFP column (150 mm × 2.1 mm, particle size 3 μm). The mobile phase consisted of 5-mM ammonium formate in water (A) and methanol (B), and the elution program was as follows: 0–1.5 min, 2% B; 1.5–3.0 min, linear increase of B from 2% to 50%; 3.0–9.0 min, B from 50% to 74%; 9.0–12.0 min, B from 74% to 95%; 12.0–15.0 min, maintain 95% B; and 15.1–21.0 min, B decreased to 2%. The temperature was controlled at 30°C, the flow rate was 0.3 mL/min, and the injection volume was 5 μL.

Mass spectrometry was performed using a HRMS (Q Exactive HF Thermo Fisher, Bremen, Germany) equipped with a heated electrospray ionization source (HESI). The collision gas (99.99% pure nitrogen) pressure was 0.2 Pa, and the sheath gas and auxiliary gas pressures (purity 99.9%) were set to 35 and 15 Pa, respectively. The capillary temperature was 320°C, and the spray voltage was +3.8 kV (ESI+). The instrument scanned simultaneously in positive and negative ion modes, with a mass error within 5 ppm, a full scan range of 100–1000 *m/z*, a resolution of 60,000 (200 *m/z*), and an AGC target value of 3×10^6; the dd-MS^2 resolution was 30,000 (200 *m/z*), and the AGC target value was 1×10^5. The collision energy gradients were 15, 40, and 70 eV, and the isolation window was 4 *m/z*.

2.6 | Metabolite Identification

Data acquisition was performed by Xcalibur 4.2 software platform. Compound Discoverer 3.3 software was used to process and analyze the acquired data to identify metabolites. Furthermore, Mass Frontier software performed detailed structural elucidation of the proposed metabolites.

2.7 | Network Pharmacology Analysis and Molecular Docking Methods

To explore the potential targets of episteride in the treatment of prostate diseases, the SMILES ID of episteride was queried using the SwissTargetPrediction database (http://swisstargetprediction.ch/), TargetNet database (http://targetnet.scbdd.com), and SuperPred database (https://prediction.charite.de). For the TargetNet database, genes with a probability score >0 were selected, whereas for the SuperPred database, genes with a model accuracy $>90\%$ and probability $>60\%$ were included.

Relevant gene information for "prostate diseases" was gathered from the GeneCards database (https://www.genecards.org/) and the OMIM database (https://omim.org/). From the GeneCards database, genes with a relevance score >20 were proposed as potential disease-related targets.

The proposed targets were uploaded to the STRING database (https://www.string-db.org/) for high-confidence Protein–Protein Interaction (PPI) network analysis. The PPI network was constructed and visualized using Cytoscape software (http://www.cytoscape.org/), and core targets were filtered based on their degree centrality values.

To perform molecular docking, the structural files of high-resolution core target proteins were retrieved from the PDB database (https://www.rcsb.org/). Protein structures were prepared using PyMol software by removing water molecules and separating ligands and receptors. Hydrogen atoms were added to the proteins using the ADFRSuite software. Grid box parameters for docking were determined using AutoDock molecular docking software, and both the small molecules and core target proteins were converted to pdbqt files using AutoDock Vina. Molecular docking simulations were then conducted to verify the interactions between episteride and its predicted targets. The docking results were visualized and analyzed using PyMol software to illustrate the binding patterns and interactions.

3 | Results and Discussion

3.1 | Metabolite Identification

In this study, the metabolic products of episteride were distinguished by comparing retention times (RT) in chromatograms and characteristic fragment ions in mass spectra. Three metabolites of episteride were detected in both in vitro human liver microsome and minipig skin microsome metabolism models, including two Phase I metabolites (M1 and M2) and one Phase II metabolite (M3). The mass deviations between the measured values and theoretical values were all within 5 ppm. The retention time of the parent compound, episteride, was 15.24 min, whereas the retention times of the metabolites were 13.52, 14.37, and 13.16 min, respectively (Figure 1 and Table 1). No parent compound or metabolites were detected in the blank control group. The metabolic transformation pathways of episteride primarily involve oxidation (M1 and M2) and glucuronidation (M3).

Under the chromatographic conditions employed in this study, episteride exhibited a retention time of 15.24 min, with a molecular ion peak of $[M+H]$ m/z 400.2835 (Figure 2). The fragment ion at m/z 344.2202, which differed from the parent drug by 56 Da, showed the second highest signal intensity after the parent drug. Based on the cleavage pattern of finasteride, this

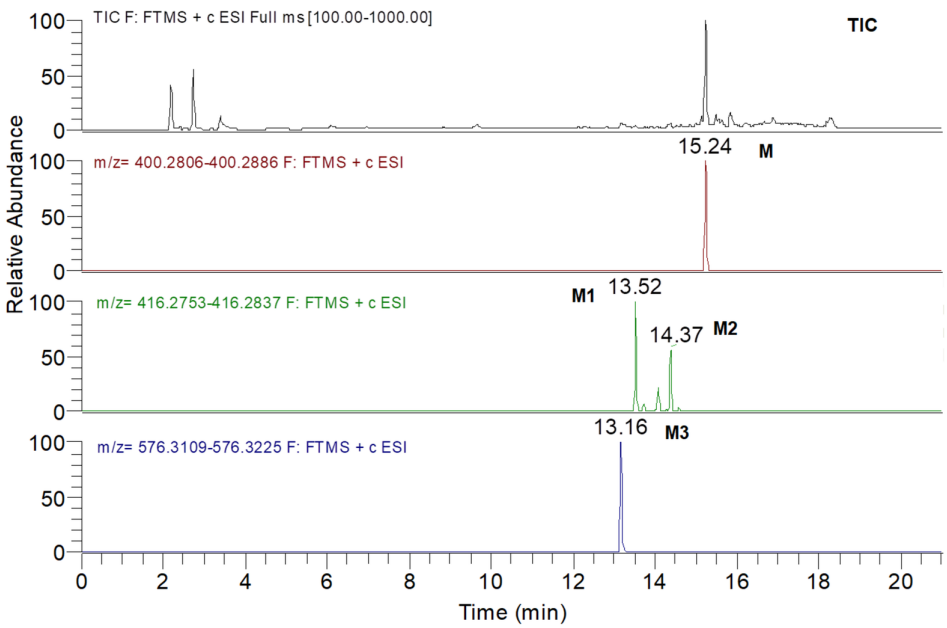

FIGURE 1 | Extracted ion chromatograms of episteride and its proposed metabolites in positive ESI mode.

TABLE 1 | Proposed metabolites of epristeride in HLMs and minipig (SMs) model.

Compound	Biotransformation	RT (min)	Formula	Adduot ion	Theoretical mass (*m/z*, Da)	Actual mass (*m/z*, Da)	Error (ppm)	Production (*m/z*, Da)
M	—	15.24	$C_{25}H_{37}NO_3$	[M + H]	400.2846	400.2835	−2.75	344.2202, 157.1008, 105.0695, 72.0444
M1	Oxidation	13.52	$C_{25}H_{37}NO_4$	[M + H]	416.2795	416.2793	−0.48	360.2145, 201.0911, 74.0443
M2	Oxidation	14.37	$C_{25}H_{37}NO_4$	[M + H]	416.2795	416.2788	−1.68	343.1902, 299.2014, 189.0902, 72.0807
M3	Glucuronide conjugation	13.16	$C_{31}H_{45}NO_9$	[M + H]	576.3167	576.3146	−3.64	520.524, 400.2832, 344.2200, 326.2099, 214.4471, 72.0444

Note: The name of M1–M3. M1: (7R,10R,13S,17S)-17-(tert-butylcarbamoyl)-7-hydroxy-10,13-dimethyl-2,7,8,9,10,11,12,13,14,15,16,17-dodecahydro-1H-cyclopenta[a]phenanthrene-3-carboxylic acid or (7S,10R,13S,17S)-17-(tert-butylcarbamoyl)-7-hydroxy-10,13-dimethyl-2,7,8,9,10,11,12,13,14,15,16,17-dodecahydro-1H-cyclopenta[a]phenanthrene-3-carboxylic acid. M2: (10R,13S,17S)-17-((1-hydroxy-2-methylpropan-2-yl)carbamoyl)-10,13-dimethyl-2,7,8,9,10,11,12,13,14,15,16,17-dodecahydro-1H-cyclopenta[a]phenanthrene-3-carboxylic acid. M3: 6-(((10R,13S,17S)-17-(tert-butylcarbamoyl)-10,13-dimethyl-2,7,8,9,10,11,12,13,14,15,16,17-dodecahydro-1H-cyclopenta[a]phenanthrene-3-carbonyl)oxy)-3,4,5-trihydroxytetrahydro-2H-pyran-2-carboxylic acid.

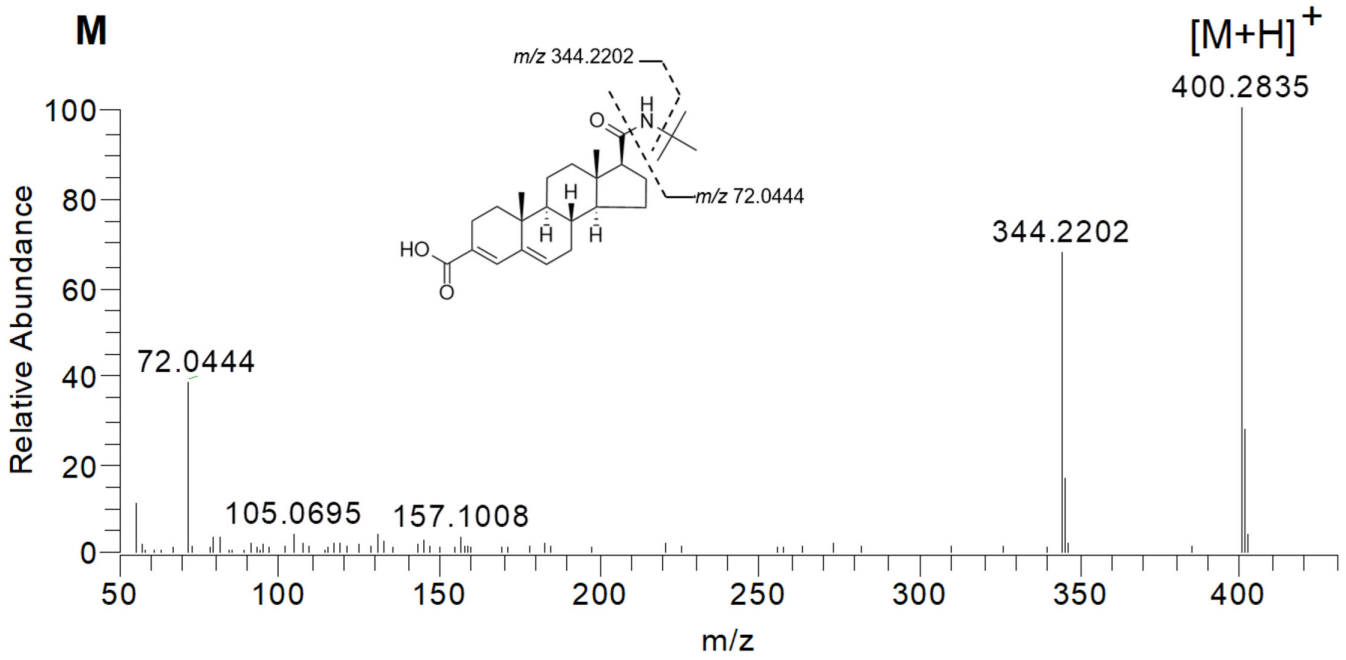

FIGURE 2 | MS spectra of epristeride with fragment ions.

fragment was inferred to result from the loss of a C_4H_8 group from the parent drug [32].

The retention times of M1 and M2 differed, but both structures were assigned by Compound Discoverer 3.3 software as having the molecular formula $C_{25}H_{37}NO_4$. The molecular ion [M + H] at *m/z* 416.2793 differed from the parent compound by 16 Da, suggesting that the parent drug underwent oxidation to form hydroxylated metabolites, designated M1 and M2 as isomers (Figures 3 and 4). In M1, the fragment ion at *m/z* 360.2145, which differed from the molecular ion by 56 Da, exhibited a cleavage pattern similar to that of the parent compound. The

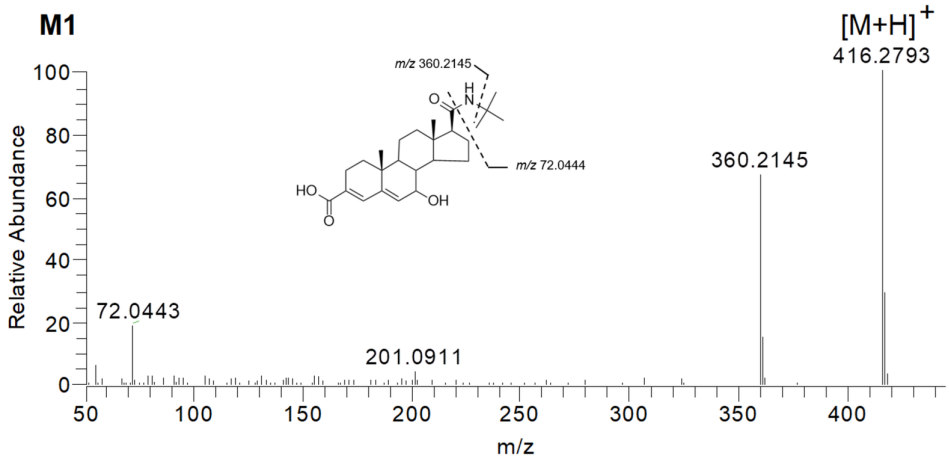

FIGURE 3 | MS spectra of M1 with fragment ions.

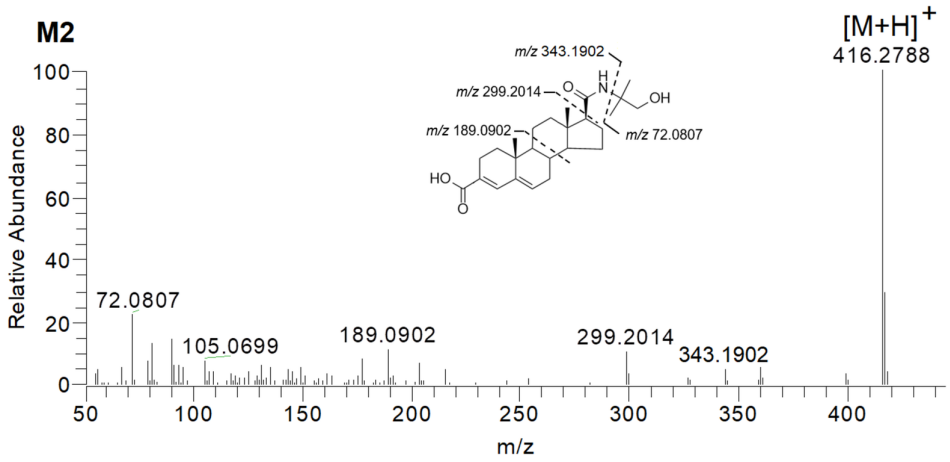

FIGURE 4 | MS spectra of M2 with fragment ions.

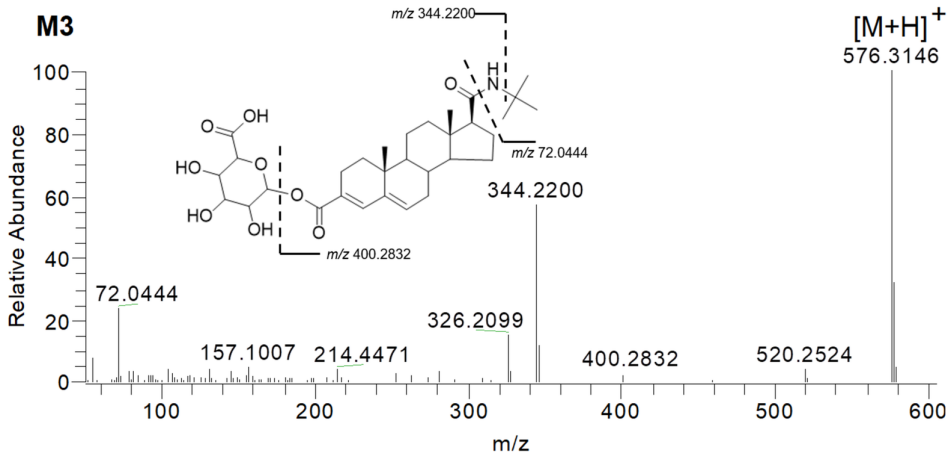

FIGURE 5 | MS spectra of M3 with fragment ions.

comparable signal intensity ratio suggests that hydroxylation occurred on the steroidal backbone. In contrast, M2 displayed fragmentation characteristics highly similar to ω-hydroxy finasteride, including the sequential loss of characteristic fragment ions corresponding to -NH_3, -C_4H_8O, -$C_5H_{11}NO_2$ [32].

The molecular ion of M3 was [M + H] *m/z* 576.3146, which differed from the parent compound by 176 Da, suggesting that it was a glucuronic acid conjugate (Figure 5). Given the presence of a carboxylic acid group in the structure of the parent drug, it was inferred that the structure involved the dehydration condensation of the carboxylic acid with glucuronic acid. The *m/z* 400.2832 corresponded to the parent drug fragment formed after the loss of glucuronic acid from M3. Additionally, the signal at *m/z* 344.2200, which was the second most intense after the molecular ion, was consistent with the fragmentation pattern of the

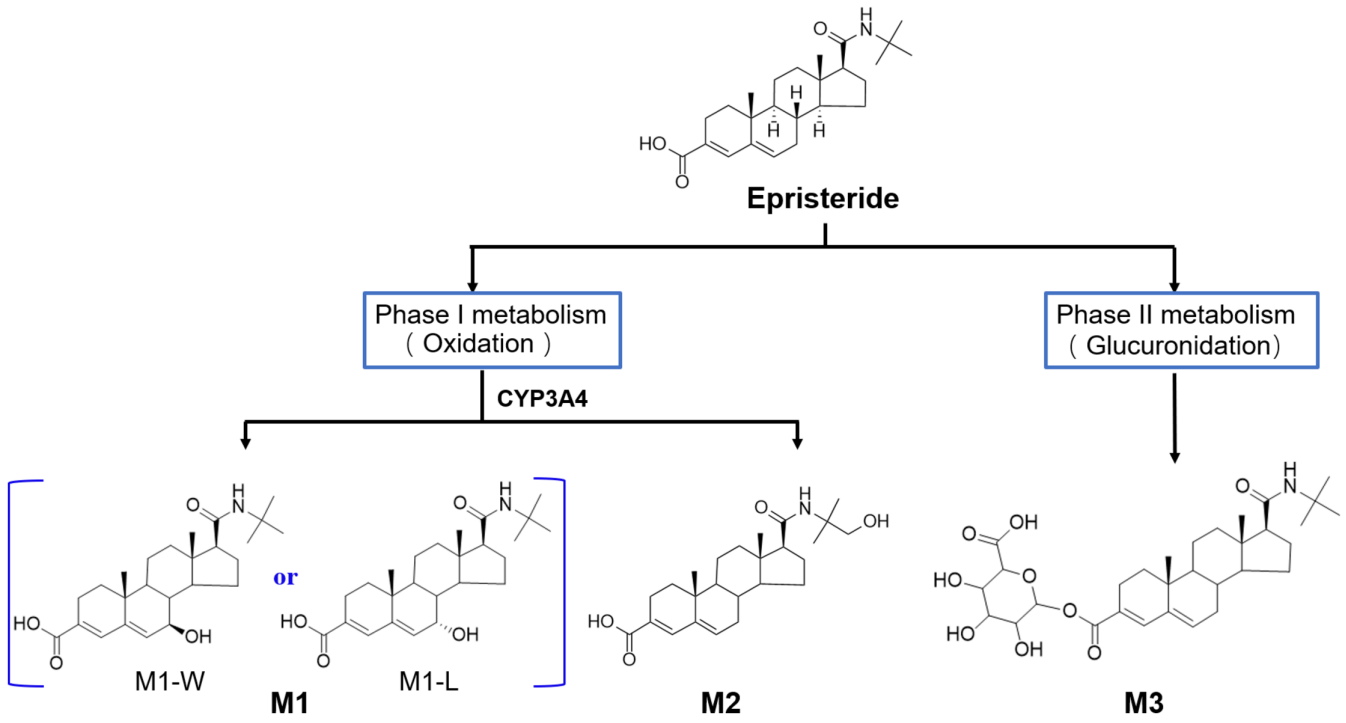

FIGURE 6 | Preliminary metabolic profile of episteride in human liver microsome and minipig skin microsome model.

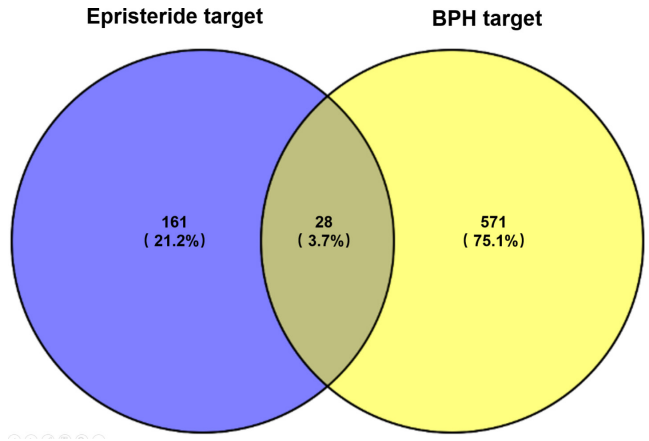

FIGURE 7 | The Venn Diagram for Predicting Targets.

parent drug, indicating the loss of a C_4H_8 from the parent drug fragment.

3.2 | Metabolic Pathway Analysis

In this study, specific inhibitors for five CYP450 isoforms including CYP2D6, CYP2C9, CYP1A2, CYP2B6, and CYP3A4 were employed to investigate their roles in the metabolic pathways of episteride. The inhibitors were added to a liver microsomal metabolism system, and the peak areas of episteride were compared before and after inhibitor addition to assess the contribution of each isoform to episteride metabolism. The results (as shown in Figure 6) revealed significant differences in catalytic efficiency among the isoforms following the addition of inhibitors. The catalytic inhibition rates for CYP2D6, CYP2C9, and CYP2B6 were all below 8%, suggesting minimal involvement of these isoforms in episteride metabolism. In contrast, CYP3A4 exhibited a substantially higher catalytic inhibition rate of 82.42%, indicating its predominant role. This finding aligns with the review by Gupta et al. [17] which reported that the hydroxylation of finasteride is primarily catalyzed by CYP3A4 [34]. Together, these results confirm that CYP3A4 plays a dominant role in the metabolism of episteride.

3.3 | The Potential Impact of Drug Metabolism on Doping Testing During Disease Treatment

Using the SMILES structure of episteride, potential targets were predicted using three databases: SwissTargetPrediction (112 targets), TargetNet (19 targets), and SuperPred (76 targets). After merging and removing duplicate entries, a total of 189 unique target genes were tentatively elucidated for episteride. To further refine the analysis, genes associated with benign prostatic hyperplasia (BPH) were retrieved from the GeneCards database (417 genes) and the OMIM database (216 genes). Following the removal of duplicates, 599 unique BPH-related genes were tentatively elucidated. By intersecting these with episteride's predicted targets, 28 potential therapeutic targets were tentatively elucidated (Figure 7).

These 28 targets were then analyzed using the STRING database, with a high-confidence interaction score threshold of 0.9, to construct a preliminary protein–protein interaction (PPI) network (Figure 8). The network was further processed using Cytoscape software to identify the top five core targets based on their degree values (degree ≥ 6). The core targets tentatively elucidated were ESR1, CYP19A1, STAT3, AKR1C3, and CYP17A1, highlighting their potential significance in the pharmacological action of episteride.

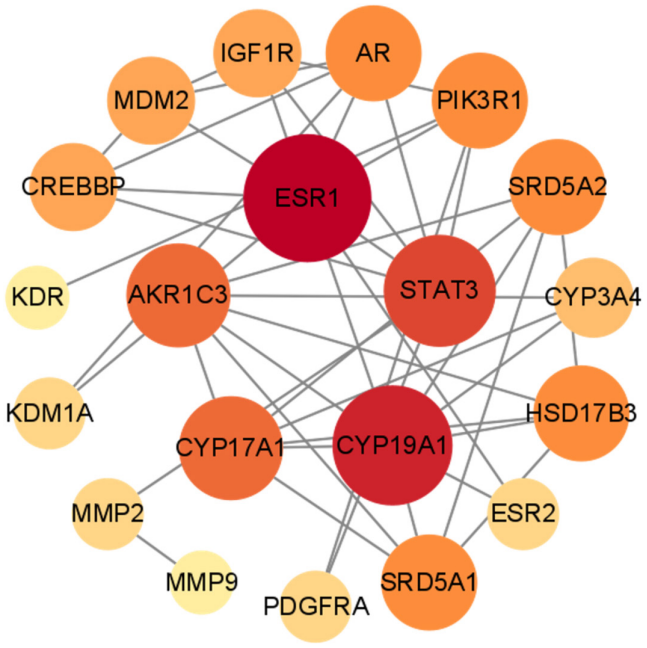

FIGURE 8 | Protein–protein interaction (PPI) network.

TABLE 2 | Results of small molecule docking with protein targets.

Compounds	CYP17A1/ energy (kcal)	CYP19A1/ energy (kcal)
Finasteride	−10.6	−8.8
Dutasteride	−11.6	−4.4
Epristeride-M	−9.9	−9.1
Epristeride-M1-W	−9.6	−8.8
Epristeride-M1-L	−9.4	−8.4
Epristeride-M2	−9.9	−8.5
Epristeride-M3	−10.4	−0.5

Based on the identification of five core therapeutic targets, CYP17A1 is a key enzyme in steroidogenesis, playing a pivotal role in the biosynthesis of steroid hormones. It has emerged as a critical target for the treatment of hormone-dependent cancers, including prostate cancer. In particular, significant efforts within the pharmaceutical chemistry field have been dedicated to the discovery and development of CYP17A1 inhibitors, especially for addressing castration-resistant prostate cancer [36–38]. Similarly, CYP19A1, also known as aromatase, is essential for converting androgens into estrogens. In cholangiocarcinoma (CCA), CYP19A1 expression is closely associated with estrogen-related proteins, such as estrogen receptors (ERα, ERβ, and GPR30) and estrogen-responsive proteins (e.g., TFF1). High levels of CYP19A1 expression have been correlated with tumor metastasis and are positively linked to GPR30 expression. Notably, in male CCA patients, elevated CYP19A1 expression in tumor tissues is associated with shorter survival times, underscoring its clinical significance.

To explore the interaction of finasteride, dutasteride, epristeride M, and its metabolites (M1 with L and W, M2 and M3) with CYP19A1, molecular docking studies were performed using AutoDock Vina software and the CYP19A1 protein structure (PDB ID: 3S79) [39]. The results (Table 2) revealed that most compounds except for dutasteride and the Phase II metabolite of Epristeride M3 exhibited favorable binding affinities (docking scores < −5 kcal/mol), indicating stable interactions characterized by tight hydrophobic interactions and hydrogen bonding. Among these, M3 had the weakest binding affinity, with a docking score of −0.5 kcal/mol. Although M3 formed a salt bridge with the protein, this interaction was significantly weakened due to the large size of its terminal acyloxy group, which impeded its ability to fit into the protein's binding pocket. Consequently, the inhibitory effect of epristeride on CYP19A1 decreases during its metabolism to the Phase II metabolite M3.

CYP17A1 and CYP19A1 are key enzymes in the steroid biosynthesis pathway, playing essential roles in the metabolism of both endogenous and synthetic steroids. Their activity and inhibition have significant implications in doping control. CYP17A1 is a central enzyme in steroidogenesis, particularly in the synthesis of androgens and progestogens. In doping control, the inhibition of CYP17A1 can alter the metabolism of endogenous steroids and potentially lead to misinterpretation of results, including false positives or false negatives in doping tests [40, 41]. Similarly, CYP19A1, also known as aromatase, is the enzyme responsible for converting androgens into estrogens. The activity of CYP19A1 directly influences the androgen-to-estrogen ratio in urine, a key marker for detecting the use of anabolic steroids. Changes in CYP19A1 activity can therefore critically impact the accuracy of doping control analyses, underscoring its importance in the regulatory framework [14, 42, 43]. These findings highlight the necessity of studying these enzymes to ensure accurate and reliable doping detection methods.

According to the docking results of epristeride and its metabolites (Figure 9), epristeride and its metabolites M1 (M1-L and M1-W) and M2 demonstrate strong binding affinity with CYP19A1, suggesting their potential to effectively inhibit the enzyme's activity. Such inhibition could significantly impact estrogen production, potentially altering the outcomes of doping tests by affecting the androgen-to-estrogen ratio. In contrast, the Phase II metabolite M3 exhibits weak binding affinity with CYP19A1, likely due to its larger molecular structure, which hinders proper fitting into the enzyme's active site. Although M3's interaction with CYP19A1 might partially influence enzyme activity, its effect is limited by the increased distance between the metabolite and critical residues within the binding pocket. Consequently, when epristeride is metabolized into its second-phase metabolite, its inhibitory effect on CYP19A1 is almost entirely diminished, allowing the metabolism of endogenous steroid hormones to gradually normalize. Compared with existing 5α-reductase inhibitors, such as finasteride and dutasteride, and known CYP17A1 and CYP19A1 inhibitors, epristeride and its metabolites exhibit comparable or even stronger inhibitory activity. This highlights the necessity of including new reductase inhibitors like epristeride in the scope of doping control measures to address their potential

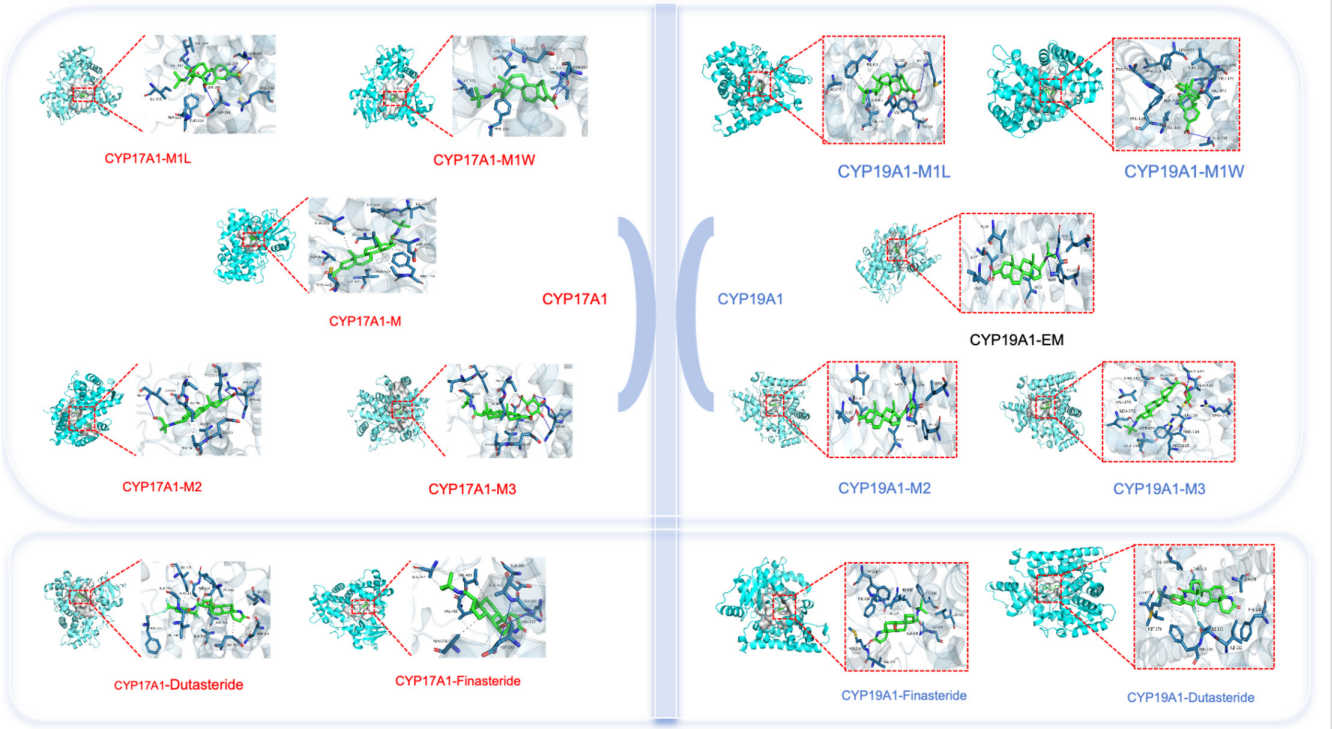

FIGURE 9 | The result diagram of compound docking with core targets.

impact on steroid metabolism and the accuracy of doping test results.

4 | Conclusion

This study investigated the in vitro metabolic characteristics of epristeride, a novel noncompetitive Type II 5α-reductase inhibitor. Utilizing human liver and minipig skin microsomal models in combination with LC-HRMS technology, the metabolic behavior of epristeride was systematically analyzed. The findings revealed the formation of three primary proposed metabolites: two Phase I oxidized metabolites (M1 and M2) and one Phase II glucuronidated metabolite (M3). Notably, CYP3A4 was tentatively elucidated as the predominant enzyme responsible for Phase I metabolism, highlighting a key role in the biotransformation of epristeride. This study not only deepens our understanding of epristeride's metabolic profile but also provides critical insights into its pharmacological mechanisms and therapeutic optimization. Additionally, network pharmacology analysis and molecular docking simulations revealed that epristeride and its metabolites interact with key steroidogenic enzymes, CYP17A1 and CYP19A1, potentially influencing steroid metabolism pathways. These interactions could impact the outcomes of doping tests, emphasizing the importance of epristeride in the field of antidoping research. Furthermore, additional insights from administration studies in humans will be critical to validate the present in vitro findings. Such investigations will help confirm the metabolic pathways, establish reliable urinary markers, and define the extent to which epristeride interferes with the steroid module of the Athlete Biological Passport. These future studies will provide essential translational evidence to complement the current work and enhance its applicability in doping control.

Author Contributions

Zhongquan Li: research concept, literature review, statistical analysis, writing – draft. **Bing Liu:** conceptualization, research concept, project administration, writing – review and editing. **Yirang Wang:** data collection, data analysis and interpretation, visualization. **Jiahui Cheng:** data analysis and interpretation, visualization, writing – draft. **Rodrigo Aguilera:** supervision, writing – review. **Xiaojun Deng:** supervision, writing – review. **Qing Chen:** theoretical computation, visualization, writing – review. **Peijie Chen:** supervision, writing – review, project administration. All authors have read and agreed to the published version of the manuscript.

Acknowledgements

The authors acknowledge the financial support of the Research Project of Shanghai University of Sport (2025STD004), Ministry of Science and Technology of the People's Republic of China (2020YFF0304500), and the World Anti-Doping Agency (WADAGrant 252C03BL). The authors thank Dr. Xavier de la Torre for the scientific support. The authors wish to thank anonymous reviewers for their constructive comments on the presentation of this article.

Conflicts of Interest

The authors declare no conflicts of interest.

Data Availability Statement

The data that support the findings of this study are available from the corresponding author upon reasonable request.

References

1. S. Simões, B. Vitoriano, C. Manzoni, and X. de la Torre, "5-Alpha Reductase Inhibitors Detection in Doping Analyses," in *Recent Advances in Doping Analysis*, vol. 16, (Sport und Buch Strauß, 2005), 199–206.

2. A. Cilotti, G. Danza, and M. Serio, "Clinical Application of 5α-Reductase Inhibitors," *Journal of Endocrinological Investigation* 24, no. 3 (2001): 199–203.

3. K. R. Loughlin, "The Clinical Applications of Five-Alpha Reductase Inhibitors," *Canadian Journal of Urology* 28, no. 2 (2021): 10584–10588.

4. K. D. Kaufman and R. P. Dawber, "Finasteride, a Type 2 5α-Reductase Inhibitor, in the Treatment of Men With Androgenetic Alopecia," *Expert Opinion on Investigational Drugs* 8, no. 4 (1999): 403–415.

5. E. Stoner, "The Clinical Development of a 5α-Reductase Inhibitor, Finasteride," *Journal of Steroid Biochemistry and Molecular Biology* 37, no. 3 (1990): 375–378.

6. R. V. Clark, D. J. Hermann, G. R. Cunningham, T. H. Wilson, B. B. Morrill, and S. Hobbs, "Marked Suppression of Dihydrotestosterone in Men With Benign Prostatic Hyperplasia by Dutasteride, a Dual 5α-Reductase Inhibitor," *Journal of Clinical Endocrinology & Metabolism* 89, no. 5 (2004): 2179–2184.

7. S. V. Frye, "Discovery and Clinical Development of Dutasteride, a Potent Dual 5α-Reductase Inhibitor," *Current Topics in Medicinal Chemistry* 6, no. 5 (2006): 405–421.

8. M. A. Levy, M. Brandt, K. M. Sheedy, et al., "Epristeride Is a Selective and Specific Uncompetitive Inhibitor of Human Steroid 5α-Reductase Isoform 2," *Journal of Steroid Biochemistry and Molecular Biology* 48, no. 2–3 (1994): 197–206.

9. E. J. Robinson, A. T. Collins, C. N. Robson, and D. E. Neal, "Effects of a New 5α-Reductase Inhibitor (Epristeride) on Human Prostate Cell Cultures," *Prostate* 32, no. 4 (1997): 259–265.

10. S. Chen, C. Li, and G. Qiang, "The Mechanism of Lingze Tablets in the Treatment of Benign Prostatic Hyperplasia Based on Network Pharmacology and Molecular Docking Technology," *Andrologia* 54, no. 10 (2022): e14555.

11. World Anti-Doping Agency, *Athlete Biological Passport Operating Guidelines* (World Anti-Doping Agency (WADA), 2023), https://www.wada-ama.org/sites/default/files/2023-07/guidelines_abp_v9_2023_final_eng_1.pdf.

12. M. Okano and S. Shiomura, "Effectiveness of Blood Steroidal Passport Markers for Detecting Testosterone Abuse in Asians," *Drug Testing and Analysis* 16, no. 6 (2024): 595–603, https://doi.org/10.1002/dta.3588.

13. U. Mareck, H. Geyer, G. Opfermann, M. Thevis, and W. Schänzer, "Factors Influencing the Steroid Profile in Doping Control Analysis," *Journal of Mass Spectrometry* 43, no. 7 (2008): 877–891.

14. H. Alquraini and R. J. Auchus, "Strategies That Athletes Use to Avoid Detection of Androgenic-Anabolic Steroid Doping and Sanctions," *Molecular and Cellular Endocrinology* 464 (2018): 28–33.

15. L. Iannella, C. Colamonici, D. Curcio, F. Botrè, and X. de la Torre, "5α-Reductase Inhibitors: Evaluation of Their Potential Confounding Effect on GC-C-IRMS Doping Analysis," *Drug Testing and Analysis* 13, no. 11–12 (2021): 1852–1861.

16. P. Oleksak, E. Nepovimova, M. Valko, S. Alwasel, S. Alomar, and K. Kuca, "Comprehensive Analysis of Prohibited Substances and Methods in Sports: Unveiling Trends, Pharmacokinetics, and WADA Evolution," *Environmental Toxicology and Pharmacology* 108 (2024): 104447.

17. A. K. Gupta, M. Talukder, and G. Williams, "Emerging and Traditional 5-α Reductase Inhibitors and Androgen Receptor Antagonists for Male Androgenetic Alopecia," *Expert Opinion on Emerging Drugs* 29 (2024): 1–261.

18. K. M. Knights, D. M. Stresser, J. O. Miners, et al., "In Vitro Drug Metabolism Using Liver Microsomes," *Current Protocols in Pharmacology* 74, no. 1 (2016): 7.8.1–7.8.24.

19. J. Shanu-Wilson, L. Evans, S. Wrigley, J. Steele, J. Atherton, and J. Boer, "Biotransformation: Impact and Application of Metabolism in Drug Discovery," *ACS Medicinal Chemistry Letters* 11, no. 11 (2020): 2087–2107.

20. M. Zhao, J. Ma, M. Li, et al., "Cytochrome P450 Enzymes and Drug Metabolism in Humans," *International Journal of Molecular Sciences* 22, no. 23 (2021): 12808.

21. Z. Li, B. Liu, Y. Wang, X. Xu, and P. J. Chen, "Metabolic Characterization of Vamorolone in Human Liver Microsomes: Implications for Anti-Doping," *Drug Testing and Analysis* 17, no. 8 (2025): 1167–1175.

22. J. Hakkola, J. Hukkanen, M. Turpeinen, and O. Pelkonen, "Inhibition and Induction of CYP Enzymes in Humans: An Update," *Archives of Toxicology* 94, no. 11 (2020): 3671–3722.

23. F. P. Guengerich, "Cytochrome P-450 3A4: Regulation and Role in Drug Metabolism," *Annual Review of Pharmacology and Toxicology* 39, no. 1 (1999): 1–17.

24. M. K. Parr, A. Zöllner, G. Fußhöller, et al., "Unexpected Contribution of Cytochrome P450 Enzymes CYP11B2 and CYP21, as Well as CYP3A4 in Xenobiotic Androgen Elimination—Insights From Metandienone Metabolism," *Toxicology Letters* 213, no. 3 (2012): 381–391.

25. W. Liu, Y. Chen, and Y. Xing, "Advances in Research on Genetic Polymorphism of Cytochrome P450 and Drug Metabolism," *China Biotechnology* 36, no. 12 (2016): 104–110.

26. K. Klein and U. M. Zanger, "Pharmacogenomics of Cytochrome P450 3A4: Recent Progress Toward the 'Missing Heritability' Problem," *Frontiers in Genetics* 4 (2013): 12.

27. L. S. Klyushova, M. L. Perepechaeva, and A. Y. Grishanova, "The Role of CYP3A in Health and Disease," *Biomedicine* 10, no. 11 (2022): 2686.

28. S. F. Zhou, "Drugs Behave as Substrates, Inhibitors and Inducers of Human Cytochrome P450 3A4," *Current Drug Metabolism* 9, no. 4 (2008): 310–322.

29. S. A. Smith, H. E. Colley, P. Sharma, et al., "Expression and Enzyme Activity of Cytochrome P450 Enzymes CYP3A4 and CYP3A5 in Human Skin and Tissue-Engineered Skin Equivalents," *Experimental Dermatology* 27, no. 5 (2018): 473–475.

30. Y. Ishii, H. Mukoyama, and M. Ohtawa, "In Vitro Biotransformation of Finasteride in Rat Hepatic Microsomes. Isolation and Characterization of Metabolites," *Drug Metabolism and Disposition* 22, no. 1 (1994): 79–84.

31. A. Lundahl, H. Lennernäs, L. Knutson, U. Bondesson, and M. Hedeland, "Identification of Finasteride Metabolites in Human Bile and Urine by High-Performance Liquid Chromatography/Tandem Mass Spectrometry," *Drug Metabolism and Disposition* 37, no. 10 (2009): 2008–2017.

32. A. Lundahl, Å. Tevell-Åberg, U. Bondesson, et al., "High-Resolution Mass Spectrometric Investigation of the Phase I and II Metabolites of Finasteride in Pig Plasma, Urine, and Bile," *Xenobiotica* 44, no. 6 (2014): 498–510.

33. M. Mazzarino, L. Martellone, F. Comunità, X. de la Torre, F. Molaioni, and F. Botrè, "Detection of 5α-Reductase Inhibitors by UPLC–MS/MS: Application to the Definition of the Excretion Profile of Dutasteride in Urine," *Drug Testing and Analysis* 11, no. 11–12 (2019): 1737–1746.

34. S. J. Park, M. H. Kim, and W. M. Yang, "Network Pharmacology-Based Study on the Efficacy and Mechanism of *Lonicera japonica thunberg*," *Applied Sciences* 12, no. 18 (2022): 9122.

35. X. D. Zhang, B. Liu, Y. F. Zou, et al., "An Efficient Strategy for the Rapid Exploration of Lipase Inhibitors Derived From the *Lindera* Aggregate Leaves by Utilizing Hybrid Lipase-Catalytic Zeolitic Imidazolate Framework Reactor Combined With HPLC-Q-TOF-MS/MS and Molecular Docking Techniques," *Food & Medicine Homology* (2025), https://doi.org/10.26599/FMH.2026.9420097.

36. T. M. Wróbel, F. S. Jørgensen, A. V. Pandey, et al., "Non-Steroidal CYP17A1 Inhibitors: Discovery and Assessment," *Journal of Medicinal Chemistry* 66 (2023): 6542–6566.

37. W. Kaewlert, C. Sakonsinsiri, N. Namwat, et al., "The Importance of CYP19A1 in Estrogen Receptor-Positive Cholangiocarcinoma," *Hormones & Cancer* 9, no. 6 (2018): 408–419, https://doi.org/10.1007/s12672-018-0349-2.

38. J. Eberhardt, D. Santos-Martins, A. F. Tillack, and S. Forli, "AutoDock Vina 1.2.0: New Docking Methods, Expanded Force Field, and Python Bindings," *Journal of Chemical Information and Modeling* 61, no. 8 (2021): 3891–3898, https://doi.org/10.1021/acs.jcim.1c00203.

39. O. Trott and A. J. Olson, "AutoDock Vina: Improving the Speed and Accuracy of Docking With a New Scoring Function, Efficient Optimization, and Multithreading," *Journal of Computational Chemistry* 31 (2010): 455–461, https://doi.org/10.1002/jcc.21334.

40. F. Xiao, X. Song, P. Tian, M. Gan, G. M. Verkhivker, and G. Hu, "Comparative Dynamics and Functional Mechanisms of the CYP17A1 Tunnels Regulated by Ligand Binding," *Journal of Chemical Information and Modeling* 60, no. 7 (2020): 3632–3647.

41. S. D. Burris-Hiday and E. E. Scott, "Steroidogenic Cytochrome P450 17A1 Structure and Function," *Molecular and Cellular Endocrinology* 528 (2021): 111261.

42. L. Wang, J. Li, L. Zhang, et al., "NR1D1 Targeting CYP19A1 Inhibits Estrogen Synthesis in Ovarian Granulosa Cells," *Theriogenology* 180 (2022): 17–29.

43. Y. Wang, Q. Ji, N. Cao, et al., "CYP19A1 Regulates Chemoresistance in Colorectal Cancer Through Modulation of Estrogen Biosynthesis and Mitochondrial Function," *Cancer & Metabolism* 12, no. 1 (2024): 33.